Supplement to 'Implications of dedicated seismometer measurements on Newtonian-noise cancellation for Advanced LIGO'

M. W. Coughlin,[1] J. Harms,[2,3] J. Driggers,[4] D. J. McManus,[5] N.
Mukund,[6] M. P. Ross,[7] B. J. J. Slagmolen,[5] and K. Venkateswara[7]

[1]*Division of Physics, Math, and Astronomy, California Institute of Technology, Pasadena, CA 91125, USA*
[2]*Gran Sasso Science Institute (GSSI), I-67100 LAquila, Italy*
[3]*INFN, Laboratori Nazionali del Gran Sasso, I-67100 Assergi, Italy*
[4]*LIGO Hanford Observatory, Richland, WA, 99352, USA*
[5]*OzGrav, Australian National University, Research School of Physics and Engineering,
Canberra, Australian Capital Territory 2601, Australia*
[6]*Inter-University Centre for Astronomy and Astrophysics (IUCAA), Post Bag 4, Ganeshkhind, Pune 411 007, India*
[7]*Department of Physics, University of Washington, Seattle, WA 98195, USA*

Appendix A: Power Spectral Densities

Figure 1 shows the locations of the seismometers in the vicinity of the vacuum enclosure, as well as the 10%, 50%, and 90% percentile vertical power spectral density at a variety of frequencies of interest.

Appendix B: Variability in the correlation function

Figure 2 shows the standard deviation in the measurement of $\Re(\gamma)$ between all 27 seismometers used for this study at 15 Hz. The coherences are calculated at a rate of once per day, and the standard deviation is computed from this distribution. As expected, the standard deviation is smallest near the center of the distribution, where both seismometers are most near to one another. The standard deviation is generally higher as the coherence becomes smaller.

Appendix C: Optimal Array configurations

In figure 3, we show the optimal 6 and 10 sensor arrays (left and right columns) for a seismometer and tiltmeter (top and bottom rows). As can be seen, most effective seismometers are typically located close to the tiltmeter, but a Wiener filter with N inputs does not optimally rely on the N closest seismometers to the tiltmeter. Some seismometers close to the tiltmeter are left out due to redundancy (their correlation with a combination of the other seismometers being too high, i.e., providing no new information). For the two 10 seismometer arrays, one can see though that even very distant seismometers can be effective, very likely given the task to monitor specific seismic sources located close to them.

Appendix D: Subtraction with tiltmeter as target sensor

Similar to the case of the tiltmeter subtraction, on the left of figure 4, we show the subtraction using a frequency domain Wiener filter between 10-20 Hz applied to a seismometer at the center of the array. The results are consistent with the expectations demonstrated in the top row of figure 4.

Appendix E: Timescales for Wiener filter subtraction

In Figure 5, we show the subtraction of seismometer and tiltmeter signals on a variety of timescales. Applying a filter calculated at some day to data recorded the same day, or a week, a month, or three months later, we see that subtraction performance is stable except for a signal around 19 Hz in the seismometer case. A simple change in power of the 19 Hz seismic source explains this result since subtraction of the 19 Hz signal is limited by sensor noise, i.e., the change in subtraction residuals only shows in relative residuals, not in the absolute residual spectrum. In general, variation in subtraction performance could also be due to changes of seismic correlations if dominant seismic sources change with time. In the tiltmeter case, no difference is seen.
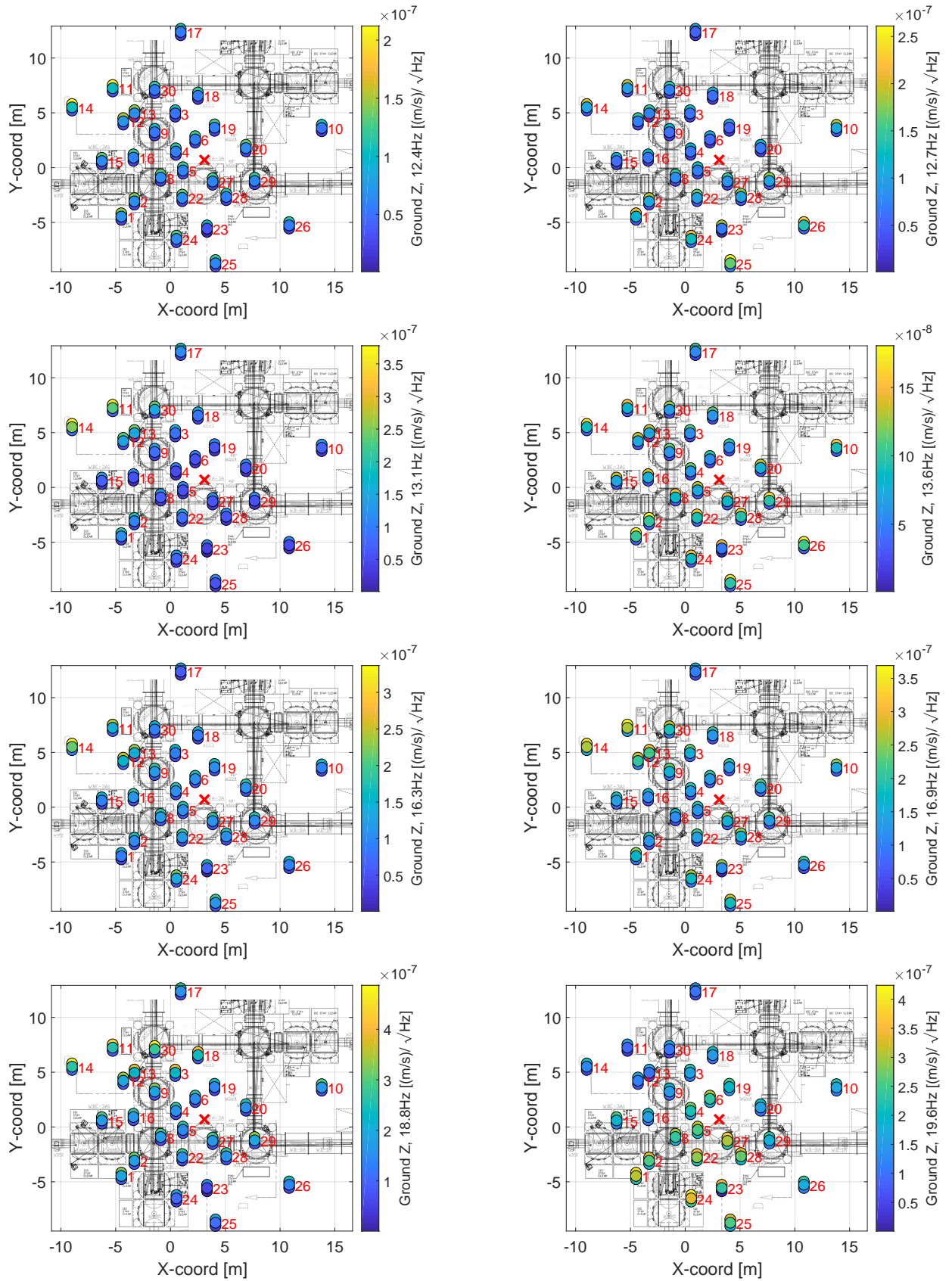
References

FIG. 1: Layout of the instrument floor at the corner station of the LIGO Hanford Observatory. The set of colored circles indicate placement of seismometers in the vicinity of the vacuum enclosure. At each set, the 10%, 50%, and 90% percentile vertical power spectral density is indicated from bottom to top. The frequencies shown are 12.4, 12.7, 13.1, 13.6, 16.3, 16.9, 18.8, and 19.6 Hz.
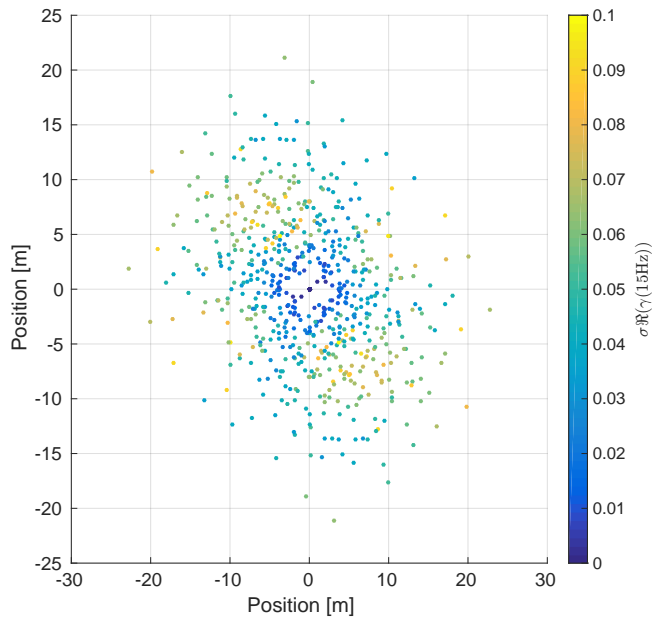
FIG. 2: Standard deviation in the measured coherence for the LIGO Hanford corner station at 15 Hz. Individual samples of coherence used to determine the standard variation are averages over one day.
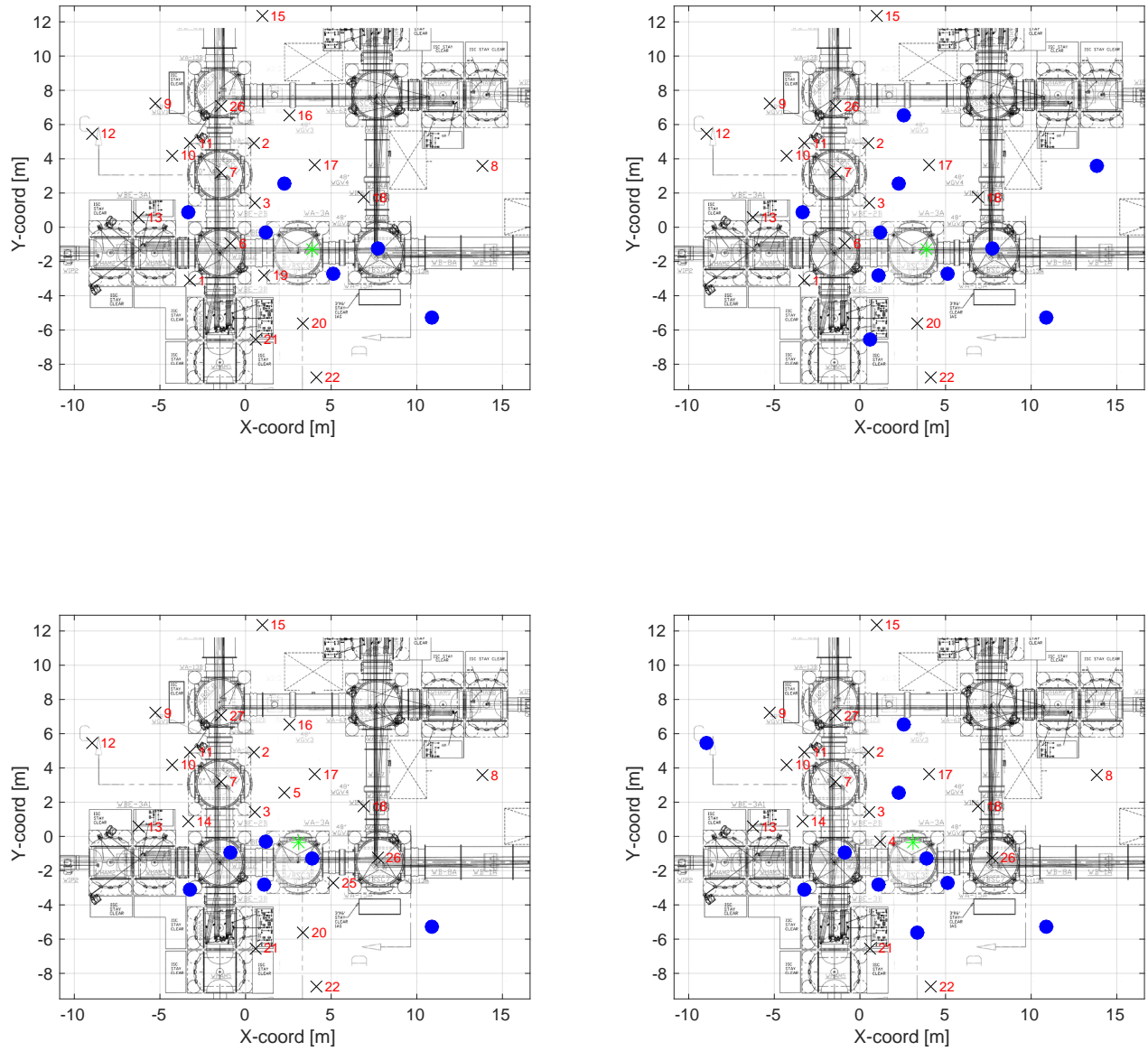
FIG. 3: Optimal 6 and 10 sensor arrays (left and right columns) for a seismometer and tiltmeter (top and bottom rows). The large blue circles indicate the locations of the seismometers that are the optimal witness sensors, while the green star is the location of the target sensor (seismometer or tiltmeter).
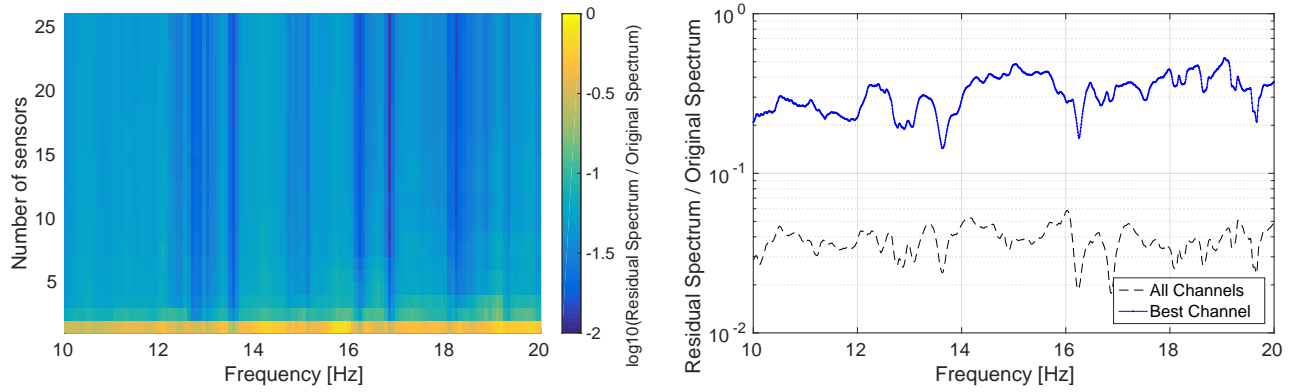
FIG. 4: On the left is the expected residuals based on Equation (1) of the letter, using the center seismometer as target and using all other seismometers in the array as witnesses. On the right is the ratio of the auto power spectral density before and after Wiener filter subtraction.
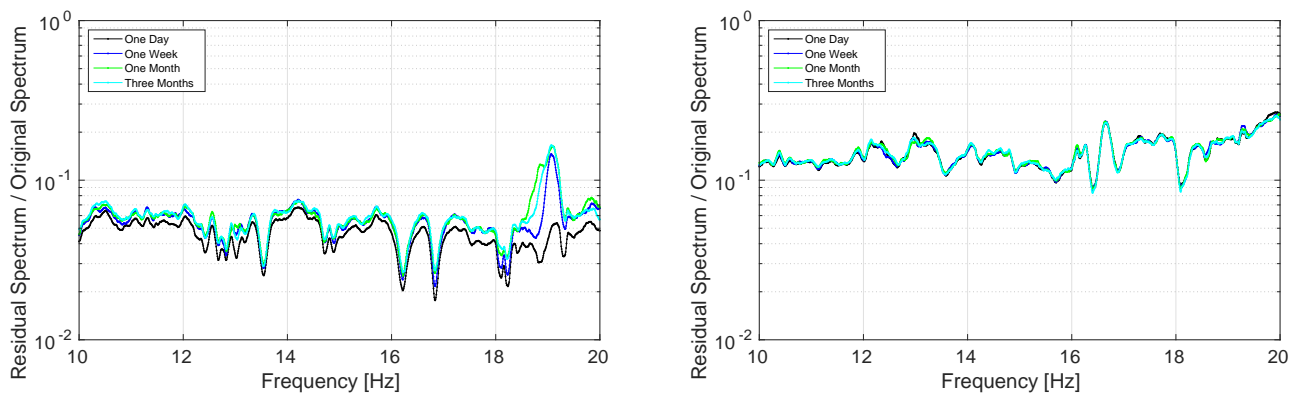

FIG. 5: Suppression of a seismometer (left) and tiltmeter (right) applying the same Wiener filter to different days after the day used for the calculation of the Wiener filter.